Mon. Not. R. Astron. Soc. **300,** 205–220 (1998)

Tidally induced star formation in Abell 1367

C. Moss,[1]★† M. Whittle[2] and J. E. Pesce[3]
[1]*Institute of Astronomy, Madingley Road, Cambridge CB3 0HA*
[2]*Department of Astronomy, University of Virginia, Charlottesville, VA 22903, USA*
[3]*Department of Astronomy and Astrophysics, Pennsylvania State University, PA 16802, USA*

Accepted 1998 June 5. Received 1998 May 6; in original form 1997 August 20

ABSTRACT

Our principal aim is to compare global star formation rates between cluster galaxies and field galaxies in order to clarify environmental influence on star formation. We use an objective prism technique to survey over 200 Zwicky catalogue (CGCG) galaxies within $\sim 2\overset{\circ}{.}5$ of Abell 1367 for Hα emission. After a brief discussion of the survey characteristics, we consider first the dependence of Hα detection on Hubble type, galaxy disturbance and the presence of a bar. As expected, we rarely detect early-type galaxies and consequently restrict further discussion to spirals (type S0/a and later), of which we detect $\sim$35 per cent in Hα. We find that an extremely valuable distinction to make is between galaxies with diffuse Hα and galaxies with compact Hα. There is a very significant tendency for galaxies with compact Hα emission to be disturbed, and there may be a weak tendency for them to be barred. Neither of these tendencies is found for galaxies with diffuse Hα emission. We infer that compact emission results from tidally induced star formation, while diffuse emission results from more normal disc star formation.

After considering field contamination, we adopt as a 'predominantly cluster' sample the spiral population inside 0.5 $r_{\rm A}$; a 'predominantly field' sample outside 0.5 $r_{\rm A}$; and a 'pure field' sample outside 1.5 $r_{\rm A}$. We consistently find a much larger fraction of spirals detected with compact Hα in the cluster sample compared to the field samples (e.g. 38 versus 0 per cent detected in cluster and 'pure field' samples, χ^2 significance 3.6σ). This increased fraction detected in the cluster is found for early-, mid- and late-type spirals separately. No such cluster/field differences are found for galaxies with diffuse Hα emission. We conclude that tidal perturbations are more common in the cluster than in the field, leading to a higher incidence of compact tidally triggered star formation.

By combining information on galaxy disturbance, galaxy companions, and the location of galaxies within the cluster, we have tried to identify the origin of the tidal perturbations. We find strong evidence that near-neighbour interaction plays a significant role in triggering star formation. However, we also find candidate objects near the cluster core which may be perturbed by the overall cluster tidal field, and candidate objects which may be influenced by a higher speed 'harassment' interaction between galaxies.

Key words: stars: formation – galaxies: clusters: individual: Abell 1367 – galaxies: evolution – galaxies: interactions – galaxies: spiral.

1 INTRODUCTION

Compared to nearby clusters of galaxies, distant rich clusters ($z \geq 0.4$) are found to have a higher fraction of blue, star-forming galaxies, often with unusual morphology suggestive of mergers and tidal interactions (e.g. Lavery & Henry 1988; Thompson 1988; Couch, Ellis & Sharples 1994). A detailed study of these blue galaxies in one very rich cluster has shown them to be rather normal spirals and irregulars (Dressler et al. 1994), suggesting that an earlier population of spirals in distant clusters has been depleted by the present epoch in rich clusters. In this view, spirals do not survive a rich environment but undergo drastic modification, being transformed into other Hubble types.

Although the depletion process is expected to be more common

★ Present address: Blackett Laboratory, Imperial College of Science, Technology and Medicine, Prince Consort Road, London SW7 2BZ.
† E-mail: c.m.moss@ic.ac.uk

Table 1. Plate material.

Plate no.	Code	UT date	Plate centre RA (1950)	Dec.	Filter	Emulsion	Prism	t (min)	Telescope & orientation
15272	A	1985 Apr 12	$11^h\ 42^m\ 57^s$	$+20^\circ\ 00'\ 06''$	RG 645	IIIaF	$2^\circ + 4^\circ$	90	BS E
15273	B	1985 May 12	11 43 22	+20 20 19	RG 645	IIIaF	$2^\circ + 4^\circ$	90	BS W
14077	C	1983 Apr 3	11 37 54	+19 59 18	RG 630	IIIaF	10°	75	BS E
14200	D	1983 May 3	11 41 55	+20 00 03	RG 630	IIIaF	10°	120	BS W
8882	E	1973 May 2	11 41 54	+20 07 00	WR2C	IIIaJ	...	60	PS ...

at earlier epochs, it is clearly of great interest to search for instances of this process at the current epoch. If the environmental effects on spirals in nearby rich clusters can be understood, this may significantly help to understand processes of spiral depletion in rich environments of the more distant past.

In the study of environmental effects on spirals, Abell 1367 is of particular interest. It is a rather unusual example of a rich cluster with a comparatively high fraction of spiral galaxies (Oemler 1974). In particular, near the cluster centre ($r \leq 0.5\ r_A$, see Section 4.1), there is the opportunity to study the effect of a dense environment on a significant number of spiral galaxies. Moreover, Oemler, Dressler & Butcher (1997) have suggested that this cluster may be more typical of the type of cluster at earlier epochs than spiral-poor clusters such as the Coma cluster. For example, in an $\Omega = 1$ universe, the hierarchical clustering model predicts that in general clusters at earlier epochs are assembled from many small groups, whereas present-day clusters are assembled from a few massive sub-clusters (Kauffmann 1995). The spiral depletion processes might be expected to have already operated within the massive sub-clusters, giving rise to the spiral-poor clusters of the present day. By contrast, Oemler et al. suggest that Abell 1367 may have been recently assembled from many small groups, thus forming with a significant spiral content and in a manner more typical of cluster formation at earlier epochs.

In this paper (Paper III) we extend earlier studies of Abell 1367 (Moss, Whittle & Irwin 1988, Paper I; Moss & Whittle 1993, Paper II). In Paper I we gave a detailed description of the objective prism technique for the detection and measurement of global Hα emission in cluster galaxies, pointing out its advantages in the study of environmental modification of star formation, and presented data on two clusters, Abell 347 and Abell 1367. In Paper II we made an initial comparison of star formation between cluster and field spirals, using photoelectric Hα data on Revised Shapley–Ames catalogue (RSA; Sandage & Tammann 1981) field spirals taken from Kennicutt & Kent (1983). This comparison had two important limitations. First, the methods used to detect Hα are quite different for cluster and field samples, and although these methods were shown to be approximately equivalent, there is still the possibility of systematic differences influencing the cluster/field comparison. Secondly, the significant difference in angular sizes of the CGCG (Zwicky & Herzog 1963) cluster galaxies and the RSA field galaxies raises the possibility of systematic differences in morphological typing, which may again influence the cluster/field comparison. Both of these limitations are overcome in the present study. Using additional plate material, we survey a sufficiently large area to construct our own field sample. In this case, the cluster and field samples have Hα emission and morphological types determined in an identical manner, allowing a more reliable comparison between cluster and field spirals.

Although the original survey method described in Paper I was developed using the 10° prism, this prism became unavailable and to continue the survey we were forced to use a lower dispersion $2^\circ + 4^\circ$ prism. Of the eight clusters surveyed, we observed two using the high dispersion prism, five using the lower dispersion prism, and only one, Abell 1367, using both. An important aim of the present study, therefore, is to use the data on Abell 1367 to show that our original survey methods can be extended to plates taken with the lower dispersion prism. This is important for forthcoming work on all eight clusters (Moss & Whittle, in preparation), in which we examine systematic trends in star formation as a function of cluster type.

Comparisons of star formation in cluster and field spirals using a variety of techniques have in the past produced varying conclusions, from claims of lessened star formation for cluster spirals to enhanced star formation. Most recent work supports either similar star formation (e.g. Biviano et al. 1997; Donas et al. 1990) or enhanced star formation (e.g. Moss & Whittle 1993; Gavazzi & Contursi 1994) in cluster spirals relative to the field, although earlier surveys using slit spectroscopy claimed reduced emission for cluster galaxies (e.g. Osterbrock 1960; Gisler 1978; Dressler, Thompson & Schectman 1985; Hill & Oegerle 1993). Biviano et al. have suggested that these surveys overestimated the fraction of emission-line galaxies (ELGs) in the field as a result of an unrecognized bias, whereby the apparent ELG fraction increases towards fainter magnitudes. This bias affects the field more than the cluster samples. In the present study, we wish to further investigate possible enhancement of star formation in cluster spirals, and its relation to the processes of spiral depletion in clusters.

In Section 2 we discuss the observational technique and present identifications of ELGs. This section also contains a comparison of the survey method using the intermediate dispersion $2^\circ + 4^\circ$ prism combination and the 10° prism. In Section 3 the detected emission is related to galaxy morphology, which leads to Section 4 in which the specific effect of cluster environment on emission in cluster spirals is considered. We find evidence for enhancement of emission in cluster spirals and consider possible mechanisms for the triggering of star formation. Conclusions are given in Section 5.

2 OBSERVATIONS

2.1 Plate material

Table 1 gives basic information on the plates used for the present study. Four objective prism plates (A,B,C,D in Table 1) were taken with the 61/94-cm Burrell Schmidt telescope at Kitt Peak. These comprise two somewhat different plate pairs.The first pair (A and B) were taken using the intermediate dispersion $2^\circ + 4^\circ$ prism combination, giving $\sim$780 Å mm^{-1} at Hα. The second pair (C and D) were taken using the high dispersion 10° prism, giving $\sim$400 Å mm^{-1} at Hα. Each plate pair includes exposures with the telescope east and west of the pier. This reverses the dispersion direction and, from the relative location of the Hα emission, allows a reasonably accurate measurement of the galaxy velocity (see

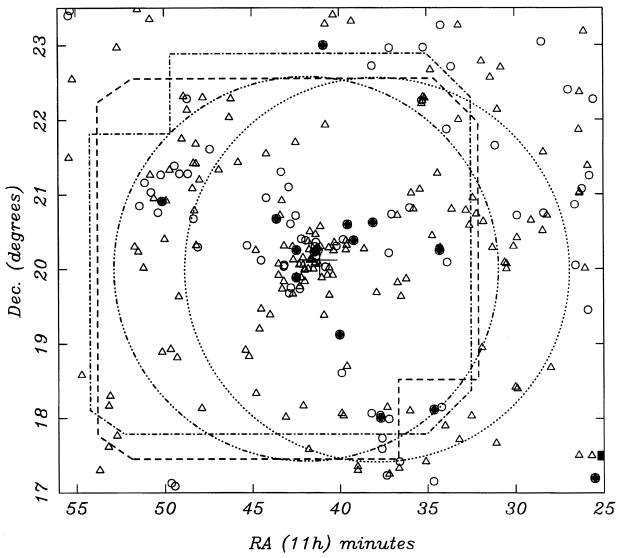

Figure 1. CGCG galaxies in the field of Abell 1367. Galaxy symbols are the same as Zwicky & Herzog (1963) : filled circles, $m_p = 13.1 - 14.0$; open circles, $m_p = 14.1 - 15.0$; open triangles, $m_p = 15.1 - 15.7$. Plate boundaries for Plate A (dashed line), Plate B (dash–dot line), Plate C (dotted line) and Plate D (dash and two dots line) are shown schematically. The centre of the cluster is shown by a cross at $11^h\ 41^m9$, $+20°\ 7'$.

Paper I and Section 2.5.3, below). All four plates were taken with unwidened spectra in conditions of good seeing and transparency, and are consequently of excellent quality.

Finally, Plate E is a direct IIIaJ+WR2C (blue) plate of 60-min exposure taken by C.D. Mackay using the 1.2-m Palomar Schmidt telescope. This excellent plate allows good morphological typing of the cluster galaxies.

2.2 Galaxies surveyed for Hα emission

We surveyed for Hα emission all CGCG galaxies within the fields of the objective prism plates. Restriction to CGCG galaxies has several advantages. First, Hα detection efficiency is approximately uniform down to the limit of the CGCG catalogue ($m_p \sim 15.7$) but drops rapidly below this limit (see Section 2.6.2, below). Secondly, it becomes increasingly difficult to assign reliable morphological types to galaxies fainter than the CGCG limit. Thirdly, the CGCG catalogue is itself thought to be complete to $m_p \sim 15.5$, and we assume that galaxies in the range $15.5 < m_p \leq 15.7$ constitute an unbiased extension below completeness. We also note that our detection efficiency will not be affected by redshift, since the highest galaxy velocities known for Abell 1367 (~ 9000 km s^{-1}, Struble & Rood 1987) are well below the redshift limit of $\sim 12\,000$ km s^{-1} set by the IIIaF emulsion cut-off (Kinman 1984).

Fig. 1 shows a schematic outline of the prism plate boundaries, each of diameter $\sim 5°$ (A and B are square, C and D are round), together with the distribution of CGCG galaxies. All CGCG galaxies are covered by one or both plate pairs out to a radial distance from the cluster centre of approximately 1.9 r_A, where r_A is the Abell radius (80 arcmin = 3 Mpc for $H_0 = 50$ km s^{-1} Mpc^{-1}, Abell 1958). Between 1.9–2.5 r_A, 26 per cent of CGCG galaxies are covered by at least one plate pair.

2.3 Galaxy types

Because global Hα emission depends on Hubble type (e.g. Kennicutt & Kent 1983), it is important to obtain accurate Hubble types in order to identify other factors which may correlate with Hα emission. The problems associated with classification of galaxies of small angular size have frequently been discussed. At a mean redshift of ~ 6000 km s^{-1}, most CGCG galaxies have sizes in the range 0.5–2.0 arcmin. Nevertheless, plate E was sufficiently good to provide reasonably reliable types for most of the galaxies.

Morphological types, classified on the revised Hubble system described by de Vaucouleurs (1959, 1974), were estimated by one of us (MW) for the majority of CGCG galaxies in the overlap region of plates C and D. Two independent classifications yielded a mean type and showed good internal consistency with typical uncertainty of ± 1 in the T class. A comparison with types estimated by Tifft (1978), who used 4-m prime focus negatives of the cluster core, shows no systematic difference in T class and rms difference of ~ 0.8 (increasing to 3.6 if uncertain types are included). Finally, a comparison with Uppsala General Catalogue (UGC) types (Nilson 1973) gives a similar level of agreement (although these constitute a subsample of larger galaxies). Although disc structure is lost in poorer plate material at smaller plate scales, the apparently large number of S0 galaxies found in the centre of the cluster is probably *not* a result of this loss of resolution – many fainter and smaller spiral galaxies are clearly visible on the plate, although these were not included in the CGCG sample.

For the remaining galaxies in the sample (mainly those outside the overlap region of plates C and D), types were independently estimated by CM and JEP using plate E or, for the few galaxies lying outside this plate, the Palomar Sky Survey O prints. The average of these two estimates was adopted as the revised Hubble type.

In addition to the type classification, a note was also made if the galaxy looked 'disturbed' in some way, including the presence of a warp or distorted spiral structure, extended plumes, or more severe signs of disturbance. Depending on the level of disturbance, a label of D, D:, or D:: was assigned, ranging from clearly disturbed to only slightly disturbed. Galaxies were also inspected for the presence of a possible nearby companion. This included galaxies closer than ~ 5 times the diameter of the sample galaxy, and larger than ~ 20 per cent of its size. Depending on the proximity and size of the companion, a label of C, C: or C:: is assigned.

2.4 Emission-line galaxy identifications

Galaxy spectra were viewed through a binocular microscope at low power ($\sim 12\times$) to identify emission-line galaxies (see Paper I for examples of such spectra). In order to eliminate spurious identifications, galaxies were not recorded as having emission unless it was visible on both plates of either plate pair. Outside the overlap region of a plate pair, a galaxy is recorded as having emission only when the Hα emission is so strong as to render any misidentification unlikely (these six galaxies are CGCG 126.074, 126.075, 126.091, 127.025A, 127.025B and 97.182). However, because such galaxies do not constitute an unbiased sample (they have stronger emission on average), they have not been included in the subsequent analysis of emission-line galaxy properties.

Table 2 gives morphological and emission-line information for all CGCG galaxies within the boundaries of the four prism plates. The table notes give a detailed description of the table contents. Briefly, columns 1–5 give the CGCG name, RA, Dec., radial distance, and photographic magnitude. Columns 6 – 8 give the revised Hubble type and note of disturbed appearance and possible nearby companion. Columns 9 and 10 give heliocentric redshift and reference. Column 11 gives the plates on which the galaxy is found.

Table 2. CGCG galaxies surveyed for Hα emission.

CGCG	R.A. (1950.0)	Dec.	r (r_A)	m_p	Type	Dis.	Cp.	$v_\odot$ (km s^{-1})	Ref.	Fields	Hα emission Vis.	Hα emission Conc.	Notes
(1)	(2)	(3)	(4)	(5)	(6)	(7)	(8)	(9)	(10)	(11)	(12)	(13)	(14)
126.073	11^h 28^m 21^s.0	+20° 42′ 16″	2.42	15.7	Sc:	...	...	...		C	...	...	p
126.074	11 28 23.6	+20 44 43	2.42	14.7	SBb pec	D	C	6167	1	C	S	D	p
126.075	11 28 26.6	+20 30 42	2.39	15.4	SB...	...	...	4217	1	C	S	N	p
126.081	11 29 12.0	+20 40 44	2.27	15.2	SABb	D::	...	...		C	...	...	p
97.001	11 29 56.4	+18 25 24	2.47	15.5	S...	...	C	...		C	...	...	
97.002	11 29 53.8	+20 25 56	2.13	15.4	S0:	?	...	...		C	...	...	p
126.083	11 30 4.6	+20 42 55	2.13	14.9	SBbc	...	...	6052	5	C	...	...	p
97.003	11 29 59.8	+18 25 8	2.47	15.5	S0/a:	...	C	12300	1	C	...	...	
97.005	11 30 10.3	+20 18 52	2.07	15.5	S0/a: pec	D:	...	6122	5	C	...	...	p
97.007	11 30 29.7	+20 0 54	2.01	15.5	S0	...	...	...		C	...	...	p
97.008	11 30 34.6	+20 4 8	2.00	15.7	S...	D:	C	9780	7	C	...	...	p
97.009	11 30 37.0	+20 5 33	1.99	15.6	Sc-Irr	D:	C	...		C	...	...	p
126.091	11 31 7.9	+21 39 24	2.21	14.4	SAbc	...	...	6583	1	C	S	VD	
97.011	11 31 13.9	+20 18 9	1.89	15.6	SAb	D::	C:	...		CD	...	...	p
126.097	11 31 58.8	+20 38 48	1.79	15.5	E–S0	...	...	...		CD	...	...	
97.013	11 31 58.1	+18 57 31	1.96	15.6	S:...	...	...	...		C	...	...	
126.100	11 32 16.8	+20 45 53	1.76	15.6	SB:ab	D::	...	...		[A]CD	...	...	
126.102	11 32 31.3	+20 57 13	1.76	15.7	Sa pec	D:	C::	...		ACD	...	...	
97.017	11 32 31.8	+18 3 20	2.27	15.7	S0	...	C:	3450	6	C	...	...	
126.103	11 32 46.6	+20 35 20	1.65	15.7	S0/a	D::	...	10300:	2	ABCD	M	VD	
126.104	11 32 58.4	+20 46 57	1.65	15.6	SAB... pec	D::	...	6679	5	ABCD	S	D	
97.018	11 33 15.2	+17 43 26	2.36	15.7	SBa	...	...	3353	6	C	...	...	
126.106	11 33 20.6	+21 59 58	2.06	15.6	E–S0	...	...	...		ABC	...	...	
126.108	11 33 43.5	+20 47 56	1.53	15.5	S0:	...	...	6555	1	ABCD	...	...	
97.021	11 33 52.1	+20 5 15	1.42	14.6	E–SA0	...	...	...		ABCD	...	...	
126.110	11 33 52.4	+21 52 24	1.93	14.8	Sab pec	D::	...	8890	1	ABC	S	C	*
97.022	11 34 3.9	+17 55 10	2.16	15.2	SB:0	...	...	8147	1	C	...	...	
97.023	11 34 15.2	+20 16 53	1.35	15.3	SB0/a	...	C	...		ABCD	...	...	
127.002	11 34 16.7	+21 16 49	1.60	15.5	Sa pec	D:	...	...		ABCD	...	...	
97.025A	11 34 18.4	+18 9 53	1.99	(15.1)[c]	E	?	C	...		BC	...	...	*
97.025B	11 34 17.6	+18 10 2	1.99	(17.0)[c]	S:...	D:	C	3341	6	BC	...	...	*
97.026	11 34 18.0	+20 14 52	1.34	13.9	SBa pec	D	C	6195	1	ABCD	S	N	
97.027	11 34 17.9	+20 16 25	1.35	14.6	SB:a pec	D	C	6630	5	ABCD	...	...	
97.030	11 34 38.4	+18 6 57	1.98	13.7	SA0	...	...	3301	1	BCD	...	...	
97.033	11 34 59.7	+20 26 25	1.24	15.6	SB:a	...	...	7137	1	ABCD	...	...	
127.005	11 34 54.1	+22 40 39	2.28	15.4	Scd:	...	...	6878	1	B	...	...	
127.006	11 35 7.1	+22 17 13	2.01	15.3	SBab	...	C	9022	1	ABC	...	...	
127.007	11 35 12.5	+22 18 11	2.01	15.5	S0/a	...	C	8992	1	ABC	...	...	
127.009	11 35 15.1	+22 15 6	1.98	15.2	E–S0	...	C	9081	1	ABC	...	...	
127.010	11 35 22.0	+21 3 19	1.35	15.7	S0	...	...	...		ABCD	...	...	
127.011	11 35 16.0	+22 4 34	1.87	15.3	E–S0	...	...	9592	5	ABC	...	...	
127.012A	11 35 17.2	+22 15 32	1.98	(15.3)[a]	Sc:	D	C	8727	1	ABC	...	...	
127.012B	11 35 18.4	+22 15 46	1.98	(15.4)[a]	SAb	D	C	8977	1	A[B]C	...	...	
127.013	11 35 46.7	+20 48 6	1.19	15.5	S0	...	C:	...		ABCD	...	...	
127.014	11 35 48.8	+21 1 1	1.27	15.2	SAcd	...	...	3357	1	ABCD	...	...	
97.035	11 36 0.1	+18 5 58	1.84	15.2	S0/a	...	...	...		BCD	...	...	
127.015	11 35 53.3	+20 48 16	1.18	14.9	E–S0	...	C:	...		ABCD	...	...	
97.036	11 36 14.8	+19 52 41	1.02	15.7	S0/a	...	...	...		ABCD	...	...	
97.037	11 36 31.6	+19 38 24	1.02	15.6	S0	...	...	...		[A][B][C][D]	?	?	
127.016	11 36 40.2	+20 42 17	1.02	15.6	Sa:	...	...	...		ABCD	...	...	
97.041	11 36 48.3	+19 48 41	0.93	15.5	SAa:	...	...	6708	1	ABCD	...	...	
127.017	11 37 1.8	+20 43 54	0.97	14.7	E–S0	...	...	7055	4	ABCD	...	...	
97.043	11 37 11.5	+17 59 18	1.81	14.5	S0/a	...	...	3434	1	ABCD	...	...	
97.044	11 37 11.5	+20 12 39	0.83	14.2	SBb	...	C:	10964	1	ABCD	M	VD	
97.046	11 37 18.2	+18 9 31	1.68	15.7	S0	...	...	...		ABCD	...	...	
97.048	11 37 36.0	+17 35 18	2.05	14.3	Sab	...	...	3527	1	AC	...	...	
97.050	11 37 40.3	+17 44 0	1.94	14.6	SA0	...	...	3297	5	ACD	...	...	
97.051	11 37 41.1	+18 0 18	1.75	13.3	S0:	D:	C	3254	1	ABCD	...	...	
97.052	11 37 43.0	+18 2 33	1.73	14.7	S...	...	C	3230	1	ABCD	...	...	
97.053	11 37 50.3	+19 41 31	0.79	15.7	S... pec	D	...	...		ABCD	...	...	

Table 2 – *continued*

CGCG	R.A. (1950.0)	Dec.	r (r_A)	m_p	Type	Dis.	Cp.	$v_\odot$ (km s^{-1})	Ref.	Fields	Hα emission Vis.	Hα emission Conc.	Notes
97.054	11^h 38^m 10^s.9	+18° 4′ 20″	1.67	14.6	SABbc	…	…	3495	5	ABCD	…	…	
127.024	11 38 5.7	+20 37 14	0.77	13.8	SB0	…	…	6472	1	ABCD	…	…	
127.025A	11 38 7.8	+22 42 27	2.05	(14.3)[a]	Sab: pec	D	C	7078	1	B	MS	D	
127.025B	11 38 8.3	+22 43 29	2.06	(15.9)[a]	S:...	D	C	7125	1	B	S	VC	
97.055	11 38 46.5	+20 14 24	0.56	15.3	E–S0	…	…	6554	1	A[B][C]D	…	…	
97.060	11 39 12.3	+20 22 52	0.52	13.6	S0/a pec	D:	…	5548	1	ABCD	…	…	
97.061	11 39 37.3	+18 40 50	1.15	15.5	E-SA0	…	…	…		ABCD	…	…	
97.062	11 39 38.9	+20 15 13	0.41	15.5	Sa: pec	D	…	7752	1	ABCD	MS	N	
97.063	11 39 39.9	+20 19 34	0.43	15.7	S... pec	D	…	6102	1	ABCD	…	…	
97.064	11 39 38.8	+20 22 31	0.44	15.6	SA0	…	C:	5968	5	ABCD	…	…	
127.032	11 39 33.2	+20 35 35	0.55	13.8	SAB0	…	C::	5600	1	ABCD	…	…	
97.066	11 39 51.0	+18 2 16	1.60	15.7	S...	…	C:	…		ABCD	…	…	
97.067	11 39 53.9	+18 36 31	1.19	14.3	SB:c pec	…	…	918	1	ABCD	S	C	*
97.068	11 39 48.7	+20 23 50	0.43	14.7	SBc pec	D:	C:	5976	1	ABCD	S	N	
97.069	11 39 56.1	+18 3 40	1.58	15.6	S0	…	C:	…		ABCD	…	…	
97.070	11 40 0.5	+19 7 20	0.82	13.6	SAa	…	…	3132	1	ABCD	S	D	
97.072	11 40 9.4	+20 18 35	0.34	15.0	SBab	…	…	6312	1	ABCD	MW	VD	
97.073	11 40 20.8	+20 14 39	0.29	15.6	SAcd: pec	…	…	7275	1	ABCD	S	D	*
97.074	11 40 23.4	+20 21 52	0.33	15.4	S0	…	…	6496	1	ABCD	…	…	
97.076	11 40 26.4	+19 55 38	0.30	15.5	SBab:	…	…	13125	1	ABCD	…	…	
97.077	11 40 42.0	+19 39 42	0.41	15.5	SB:0	…	…	6531	1	ABCD	…	…	
97.078	11 40 40.6	+20 1 35	0.23	15.2	S0	…	C:	7526	1	ABCD	…	…	
97.079	11 40 37.6	+20 16 57	0.26	15.7	S:... pec	D	…	7000	1	ABCD	S	N	*
97.082	11 40 48.9	+20 1 38	0.21	15.0	SA0/a	…	C:	6100	1	ABCD	…	…	
127.036	11 40 48.7	+21 55 43	1.37	15.5	Sbc	…	C:	3524	1	ABCD	…	…	
97.083	11 40 55.6	+19 54 19	0.24	15.2	SA0/a	D:	C:	13102	4	ABCD	…	…	
97.084	11 41 2.1	+19 22 6	0.58	15.1	E–S0	…	…	6824	4	ABCD	…	…	
97.085	11 41 1.4	+19 52 56	0.24	15.7	E-SA0	…	C:	6564	1	ABCD	…	…	
97.086	11 41 11.0	+20 18 59	0.20	15.7	S0	…	…	6399	1	ABCD	…	…	
127.040	11 41 8.5	+20 33 0	0.35	15.3	S0	…	…	6906	4	ABCD	…	…	
97.087	11 41 13.1	+20 14 50	0.16	14.3	Sd pec	D	C	6730	1	ABCD	S	N	*
97.088	11 41 24.0	+20 3 24	0.10	15.2	S0	…	C	5624	1	ABCD	…	…	
97.089	11 41 20.8	+20 10 20	0.11	14.2	E	…	…	6248	1	ABCD	…	…	
97.090A	11 41 22.0	+20 13 52	0.13	(15.6)[c]	S0	?	C	6040	1	ABCD	…	…	
97.090B	11 41 21.2	+20 13 58	0.13	(16.8)[c]	…	?	C	…		ABCD	…	…	
97.091	11 41 23.3	+20 21 17	0.20	14.7	SABb	…	…	7369	1	ABCD	S	N	
97.092A	11 41 22.6	+20 27 46	0.27	(15.8)[c]	S0 pec	D	C	6373	1	ABCD	S	N	
97.092B	11 41 22.0	+20 28 2	0.28	(17.0)[c]	…	?	C	…		ABCD	…	…	
97.093	11 41 26.3	+20 3 43	0.10	15.5	Sa:	D	C	4937	1	ABCD	MS	N	
97.094	11 41 27.6	+20 4 44	0.09	15.7	S0	…	C:	8004	1	ABCD	…	…	
97.095	11 41 26.4	+20 13 37	0.12	13.3	E	…	C	6237	1	ABCD	…	…	
97.096	11 41 26.5	+20 14 57	0.13	15.0	E–S0	…	C	6363	1	AB[C]D	…	…	
97.097	11 41 25.2	+20 18 24	0.17	14.9	S0	…	…	6834	1	ABCD	…	…	
97.099	11 41 32.1	+20 0 54	0.10	15.7	E–S0	…	C:	7733	1	ABCD	…	…	
97.100	11 41 29.9	+20 16 24	0.14	15.1	SB0	D::	C:	5640	1	ABCD	…	…	
97.101	11 41 43.4	+20 7 20	0.03	15.3	SB0	…	C	6454	1	ABCD	…	…	
97.102A	11 41 41.6	+20 30 3	0.29	(15.4)[a]	Sa	D:	C	6300	1	ABCD	…	…	
97.102B	11 41 40.9	+20 29 39	0.28	(16.8)[a]	S0	?	C	…		ABCD	…	…	
97.105	11 41 45.2	+20 6 12	0.03	15.4	SB0	…	C	5440	1	ABCD	…	…	
97.106	11 41 44.9	+20 15 31	0.11	15.2	E–S0	…	…	6469	1	ABC[D]	…	…	
97.108	11 41 48.1	+17 35 17	1.90	15.5	E–S0	…	…	3345	6	AD	…	…	
97.109	11 41 52.9	+20 0 46	0.08	15.5	S0	…	…	6823	1	ABCD	…	…	
97.110	11 41 49.6	+20 6 20	0.02	15.5	S0	…	C	4527	1	ABCD	…	…	
97.111A	11 41 49.5	+20 23 7	0.20	(15.8)[b]	S0	?	C	…		ABCD	…	…	
97.111B	11 41 50.4	+20 22 49	0.20	(16.9)[b]	S0 pec	D	C	…		ABCD	…	…	
97.112	11 41 55.0	+20 21 15	0.18	14.9	S0	…	…	6753	1	ABCD	…	…	
97.113	11 42 11.1	+20 2 7	0.08	15.6	S0	?	C:	6419	1	ABCD	…	…	
97.114	11 42 12.2	+20 3 3	0.07	15.4	S0/a: pec	D:	C:	8293	1	ABCD	S	N	
97.115	11 42 12.0	+20 9 14	0.06	15.5	S0	…	…	7792	1	ABCD	…	…	
97.116	11 42 12.2	+18 8 40	1.48	15.5	Sc:	…	…	3441	6	ABCD	…	…	

Table 2 – *continued*

CGCG	R.A. (1950.0)	Dec.	r (r_A)	m_p	Type	Dis.	Cp.	$v_\odot$ (km s^{-1})	Ref.	Fields	Hα emission Vis.	Hα emission Conc.	Notes
97.117	11^h 42^m 14.6^s	+19° 48′ 38″	0.24	15.1	SA0/a	…	…	6256	1	ABCD	…	…	
97.118	11 42 16.7	+19 53 17	0.19	15.7	S0/a	?	…	6556	1	ABCD	…	…	
97.119	11 42 12.4	+19 57 57	0.13	15.7	SB0	…	C	4869	1	ABCD	…	…	
97.120A	11 42 13.7	+20 4 21	0.06	(14.6)[b]	SAab	…	C	5000	1	ABCD	…	…	
97.120B	11 42 13.4	+20 5 7	0.06	(17.4)[b]	…	?	C	…		[A]B[C][D]	…	…	
97.121	11 42 11.5	+20 24 10	0.22	14.6	SBb pec	D::	…	6573	1	ABCD	…	…	
97.122	11 42 16.9	+19 43 55	0.30	14.9	Sb pec	D	…	5508	1	ABCD	S	N	*
97.123	11 42 20.4	+19 46 17	0.27	15.7	S0	…	…	6457	1	ABCD	…	…	
97.124A	11 42 21.5	+20 0 34	0.11	(15.6)[b]	S0	…	C	…		ABCD	…	…	
97.124B	11 42 22.1	+20 0 57	0.11	(16.9)[b]	…	?	C	…		ABCD	…	…	
97.125	11 42 19.3	+20 3 13	0.09	15.6	Sa: pec:	D:	C:	8288	1	ABCD	MS	N	
97.127	11 42 29.4	+19 52 54	0.21	14.0	E	…	C	6462	1	ABCD	…	…	
97.128	11 42 28.0	+19 53 55	0.19	15.2	E–S0	…	C	6345	1	ABCD	…	…	
97.129A	11 42 28.4	+20 15 5	0.14	(14.2)[a]	SABb	…	C	5082	1	ABCD	…	…	
97.129B	11 42 31.4	+20 14 40	0.14	(15.7)[a]	S:...	…	C	5029	1	ABCD	…	…	
127.045	11 42 30.4	+20 42 56	0.46	14.5	SAa	…	…	6878	1	ABCD	MW	D	
127.046	11 42 30.0	+21 41 23	1.18	15.6	SB:bc pec	D:	C:	7814	5	ABCD	S	N	*
97.130	11 42 40.2	+19 40 12	0.36	15.5	SA0/a	…	…	6697	1	ABCD	…	…	
97.131	11 42 39.4	+20 7 23	0.13	15.1	S0	…	…	7646	1	ABCD	…	…	
97.133A	11 42 42.2	+20 17 51	0.19	(16.4)[b]	Sb pec	D	C	5365	8	ABCD	…	…	
97.133B	11 42 41.6	+20 18 5	0.19	(16.5)[b]	S0 pec	D	C	14000	8	ABCD	…	…	
97.134	11 42 54.3	+19 40 40	0.37	14.6	SB0	…	C:	5000	1	ABCD	…	…	
97.135	11 42 54.6	+19 43 20	0.35	14.8	S0	…	…	6653	1	ABCD	…	…	
127.047	11 42 48.4	+20 36 10	0.39	14.6	SA:0	…	…	7243	1	ABCD	…	…	
127.048	11 42 52.2	+21 5 4	0.74	15.0	E–S0	…	…	6935	4	ABCD	…	…	
97.136	11 43 7.4	+18 1 29	1.59	15.4	E–S0	…	…	…		ABCD	…	…	
97.137	11 43 10.6	+20 3 4	0.23	14.2	E	…	C	5438	1	ABCD	…	…	
97.138	11 43 9.2	+20 18 33	0.26	15.5	SAc	…	…	5320	1	ABCD	W	D	
97.139	11 43 14.0	+20 2 41	0.24	14.8	S0	…	C	7088	1	ABCD	…	…	
97.140	11 43 23.4	+19 48 24	0.35	15.4	SB0	…	…	5486	1	ABCD	…	…	
127.049	11 43 13.4	+20 54 23	0.63	15.5	SBab	…	…	7060	1	ABCD	S	C	
127.050	11 43 20.1	+21 18 11	0.92	14.8	SBc	…	…	6750	1	ABCD	…	…	
127.051A	11 43 24.4	+20 43 0	0.52	(15.7)[b]	SB0/a	D:	C	7314	9	ABCD	S	C	
127.051B	11 43 24.1	+20 43 30	0.52	(16.0)[b]	Sa pec	D	C	7105	9	ABCD	…	…	
97.141	11 43 27.8	+19 42 52	0.41	15.6	SA0/a	…	…	5165	1	ABCD	…	…	
97.142	11 43 31.0	+19 54 43	0.32	15.7	S0	…	…	6357	1	ABCD	…	…	
97.143A	11 43 30.8	+20 4 4	0.28	(15.6)[b]	SB0	…	C	…		ABCD	…	…	
97.143B	11 43 28.3	+20 3 52	0.28	(16.8)[b]	…	…	C	…		ABCD	…	…	
127.052	11 43 36.8	+20 40 10	0.51	14.0	SA0	…	…	6948	1	ABCD	MW	C	
97.144	11 43 59.2	+19 23 16	0.66	15.3	S0	…	…	6158	4	ABCD	…	…	
127.054	11 44 11.8	+20 57 11	0.74	14.2	SAcd	…	…	7026	1	ABCD	…	…	
127.055	11 44 11.3	+21 32 59	1.14	15.1	SAa	…	…	6570	1	ABCD	MS	N	
97.147	11 44 30.3	+20 6 53	0.46	14.3	S0	…	…	5767	1	ABCD	…	…	
97.148	11 44 37.6	+19 12 13	0.84	15.5	SA0	…	…	11209	4	ABCD	…	…	
97.149	11 44 39.9	+19 27 14	0.70	15.6	SAa:	…	…	6060	1	ABCD	…	…	
97.151	11 44 53.1	+18 19 51	1.44	15.6	Sa:	…	…	5854	7	ABCD	…	…	
97.152	11 45 4.1	+20 13 1	0.56	15.5	SBa:	…	…	6193	1	ABCD	…	…	
97.153A	11 45 15.2	+18 49 35	1.14	(16.3)[a]	Sb pec	D:	C	…		ABCD	…	…	
97.153B	11 45 13.4	+18 49 52	1.13	(16.4)[a]	SBbc	D::	C	…		ABCD	…	…	
97.154	11 45 27.8	+18 55 37	1.09	15.7	S0/a	…	…	…		ABCD	…	…	
97.155	11 45 28.2	+20 17 3	0.64	15.0	S0	…	…	7280	1	ABCD	…	…	
127.056	11 45 52.3	+21 26 5	1.21	15.7	Sb:	…	…	6848	1	ABCD	W	VD	
127.058	11 46 13.4	+22 17 19	1.79	15.7	SBb	…	…	10329	1	ABD	MW	C	*
127.059	11 46 14.5	+22 2 4	1.62	15.6	Sb pec	D:	C:	9809	1	ABD	…	…	
127.062	11 46 55.3	+21 19 17	1.26	15.5	SB:a	…	…	…		ABCD	…	…	
127.063	11 47 24.3	+21 36 42	1.47	14.4	E–S0	…	…	7840	1	ABD	…	…	
127.066	11 47 45.7	+22 17 29	1.92	15.6	SAab	…	…	…		AB	…	…	
97.160	11 47 58.5	+18 8 10	1.83	15.6	S0/a	…	C:	6300	14	ABD	…	…	
97.161	11 48 6.5	+20 17 34	1.10	14.5	E–S0	…	C:	6244	1	ABCD	…	…	
127.067	11 48 4.6	+21 11 7	1.34	15.5	S:...	…	…	6500	14	ABD	W	VD	

Table 2 – *continued*

CGCG	R.A. (1950.0)	Dec.	r (r_A)	m_p	Type	Dis.	Cp.	$v_\odot$ (km s^{-1})	Ref.	Fields	Hα emission Vis.	Hα emission Conc.	Notes
97.162	11^h 48^m 15^s.8	+20° 19′ 36″	1.13	15.7	S0	…	C:	…		ABC[D]	…	…	
127.068	11 48 17.7	+21 26 51	1.50	15.3	S–Irr	D	C:	7705	3	ABD	…	…	
127.069	11 48 16.1	+21 40 3	1.61	15.7	S0/a	…	…	…		ABD	…	…	
127.070	11 48 16.6	+20 46 30	1.22	15.4	S0/a	…	…	…		ABCD	…	…	
127.071	11 48 20.6	+21 25 26	1.49	15.4	S... pec	D	C:	6388	5	ABD	S	N	*
127.072	11 48 26.2	+20 40 39	1.22	14.6	SABbc	…	…	6438	1	ABCD	…	…	
127.073	11 48 27.4	+21 4 40	1.35	15.1	SBab	…	…	5000	1	ABD	…	…	
127.074	11 48 39.8	+21 16 47	1.47	15.0	S0	…	…	3363	12	ABD	M	N	
127.075	11 48 46.2	+22 10 3	1.95	15.3	SAB0/a	…	C:	…		AB	…	…	
127.076A	11 48 51.6	+22 18 23	2.04	(15.5)[a]	E	?	C	8577	11	AB	…	…	
127.076B	11 48 53.3	+22 18 16	2.04	(15.5)[a]	E	?	C	7648	11	AB	…	…	
127.078	11 49 3.3	+21 44 27	1.74	15.3	S0/a	D:	…	…		ABD	…	…	
127.079	11 48 59.9	+22 20 12	2.07	15.7	S0	…	…	…		AB	…	…	
127.080	11 49 7.8	+21 16 50	1.54	14.5	E–S0	…	…	7130	1	ABD	…	…	
97.168	11 49 13.7	+19 38 9	1.34	15.7	Sbc:	…	…	7700	14	ABD	W	N	
97.169	11 49 17.8	+18 49 28	1.63	15.7	Sc	…	…	5992	1	ABD	…	…	
127.082	11 49 25.0	+21 23 13	1.62	14.7	SAc	…	…	6662	1	ABD	…	…	
97.172	11 49 39.7	+18 55 44	1.63	15.7	SABb:	…	…	…		ABD	MW	VD	
127.083	11 49 45.2	+21 22 50	1.67	15.1	Sa	…	…	6743	5	ABD	…	…	
127.085	11 49 55.9	+20 54 14	1.52	15.5	Sa	…	C:	6595	13	ABD	…	…	
97.173A	11 50 6.7	+20 25 31	1.46	(16.1)[c]	E	D::	C	…		ABD	…	…	
97.173B	11 50 6.2	+20 25 37	1.46	(16.9)[c]	…	D::	C	…		ABD	…	…	
97.174	11 50 9.4	+18 53 33	1.72	15.7	Sc:	…	…	7877	7	ABD	…	…	
127.088	11 50 7.9	+20 54 34	1.56	14.0	E–S0	…	C:	6617	5	ABD	…	…	
127.089	11 50 11.8	+21 16 3	1.69	14.3	E	…	…	6500	1	ABD	…	…	
127.090	11 50 22.1	+20 45 26	1.56	14.7	SBa	…	C::	6559	1	ABD	…	…	
127.092	11 50 36.5	+20 56 13	1.64	15.3	E–S0	…	C:	…		ABD	…	…	
127.095	11 50 45.8	+21 1 50	1.70	14.2	SBb	…	…	6199	1	ABD	M	C	
127.096	11 50 46.1	+21 17 59	1.79	15.5	SAa	…	…	…		ABD	…	…	
127.098	11 51 7.2	+21 9 38	1.79	14.4	E	…	…	6971	1	ABD	…	…	
97.176	11 51 15.7	+20 1 42	1.65	15.5	Sa	…	…	…		ABD	…	…	
127.100	11 51 25.2	+20 51 3	1.76	14.9	SBab	…	C:	6979	1	ABD	…	…	
97.178	11 51 25.3	+20 14 7	1.67	15.6	S...	…	…	6206	10	ABD	…	…	
97.180	11 51 39.5	+20 18 20	1.72	15.6	Sab	…	…	6228	1	ABD	S	D	
97.182	11 52 42.4	+17 45 57	2.60	15.4	SABb	…	…	6633	1	A	MS	N	
97.183	11 53 1.9	+18 18 27	2.39	15.5	E–S0	…	C:	…		AB	…	…	
97.185	11 53 10.4	+18 10 1	2.47	15.5	S0:	…	…	6346	5	AB	…	…	

References: 1. Huchra et al. (1992) 2. Moss et al. (1988), Paper I 3. Gavazzi et al. (1991) 4. Zabludoff, Huchra & Geller (1990) 5. de Vaucouleurs et al. (1991) 6. Lu et al. (1993) 7. Scodeggio & Gavazzi (1993) 8. Gavazzi & Randone (1994) 9. Zabludoff et al. (1993) 10. Gavazzi, Randone & Branchini (1995) 11. Karachentsev, Lebedev & Shcherbanoversuskij (1985) 12. Paturel et al. (1989) 13. Nasa Extragalactic Database 14. This paper, two plate method with mean error $\sim$ 270 km s^{-1} (see Paper I for description of method).

Notes on individual objects:

CGCG 126.110: This galaxy is Markarian 739 which has two nuclei separated by 6.6 arcsec, of which the eastern is a Seyfert 1. Spectra of both nuclei are visible on the prism plates, with emission visible from the Seyfert nucleus. A CCD direct image shows loops and a tail, indicating a merger (Keel 1996).

CGCG 97.025A & B: The radial velocity is a 21-cm measurement for the galaxy pair. It has been assumed that the radio emission originates from component B.

CGCG 97.067: The emission is from the bright concentration in the north-west part of this galaxy.

CGCG 97.073: Emission extended in plane of galaxy.

CGCG 97.079: This galaxy is listed as double by Zwicky & Herzog (1963). The galaxy components are separated by $\sim$ 9 arcsec in an east–west direction; the emission appears double with a similar separation and alignment.

CGCG 97.087: Emission is visible from four distinct regions in the plane of this edge-on galaxy.

CGCG 97.122: Emission extended in plane of galaxy.

CGCG 127.046: Emission extended in plane of galaxy.

CGCG 127.058: Double spectra indicating possible companion $\sim$ 9 arcsec to north-west of galaxy.

CGCG 127.071: Double spectra indicating possible companion $\sim$ 10 arcsec to east of the galaxy.

Table 2 – *continued*

Explanations of columns in Table 2.
Column 1. CGCG number (Zwicky & Herzog 1963).
Columns 2 and 3. Right Ascension and Declination (1950.0) of the galaxy centre accurate to approximately 2 arcsec, from Kraft Kraft1978 or measured from the PSS.
Column 4. Radial distance in Abell radii from the cluster centre ($11^h\,41^m9, +20^\circ\,7'$). The Abell radius of the cluster (3 Mpc) is assumed to be 80 arcmin, based on a mean redshift of the cluster corrected to the centroid of the Local Group, $< z_0 > = 0.0215$ (Struble & Rood, 1987, $H_0 = 50$ km s^{-1} Mpc^{-1}).
Column 5. Photographic magnitude (Zwicky & Herzog 1963). For double galaxies the CGCG value is taken for the combined magnitude, while the source for the ratio is given by the letter code : [a] PGC (Paturel et al. 1989), [b] Kraft (1978), [c] eye estimate of PSS. The estimated individual magnitudes are given in parentheses.
Column 6. Revised Hubble type (de Vaucouleurs 1959, 1974). Most types were determined from plate E. Galaxies outside plate E were classified using the PSS O print, and are noted with a 'p' in column 14 (See Section 2.3).
Column 7. Code indicating that the galaxy appears disturbed, on a 3-rank scale (D, D:, D::).
Column 8. Code indicating that the galaxy has a possible nearby companion, on a 3-rank scale (C, C:, C::).
Columns 9 and 10. Heliocentric velocity and reference.
Column 11. Plate fields (coded as in Table 1) in which the galaxy appears. A plate field enclosed in square brackets indicates that the galaxy spectrum is not visible due to being overlapped by an adjacent spectrum, or in one case (CGCG no. 126.100) due to a plate defect.
Column 12. A visibility parameter describing how readily the Hα emission is seen on the plate according to a five-point scale (S strong, MS medium-strong, M medium, MW medium-weak, W weak) weighted according to its appearance on the four plates.
Column 13. A concentration parameter describing the spatial distribution of the Hα emission and contrast with the underlying continuum, on a five-point scale (VD very diffuse, D diffuse, N Normal, C concentrated, VC very concentrated) weighted according to its appearance on the four plates.
Column 14. Notes. A 'p' indicates that the galaxy type (column 6) has been determined from PSS O prints; otherwise the galaxy type has been determined from Plate E. An asterisk indicates that a note on this galaxy appears below the table.

Columns 12 and 13 describe the appearance of the Hα emission, if seen. Column 12 gives a visibility parameter which describes how readily the Hα is seen on the plate on a five-point scale (S – strong; MS – medium-strong; M – medium; MW – medium-weak; and W – weak). Column 13 gives a concentration parameter which describes the spatial distribution of the emission and its contrast with the underlying continuum, also on a five-point scale (VC – very concentrated; C – concentrated; N – normal; D – diffuse; and VD – very diffuse). The more concentrated emission is much brighter than the underlying continuum, is sharply delineated from it, and is almost always centred on the nucleus in a small region (median diameter 3.9 kpc). The more diffuse emission is only slightly brighter than the continuum, has an indistinct appearance, and spans a larger region (median diameter 10.3 kpc). Independent determinations of the visibility and concentration parameters by different observers are in found to be in good agreement. Values given in Table 2 are the averages from all plates on which the emission is seen. Finally, column 14 indicates that a note on this galaxy appears below the Table.

2.5 Comparison of 10° prism and 2°+ 4° prism combination

Although our original survey method was developed using the 10° prism (and indeed plates C and D were part of that study), we were forced to use the 2°+ 4° prism combination for much of our cluster survey when the 10° prism became unavailable. One of the main aims of this paper, therefore, is to show that our original methods can be extended to plates taken with the lower dispersion prism.

2.5.1 Hα detection efficiency

We use the 132 CGCG galaxies with visible spectra on all four plates to test the relative Hα detection efficiency using the 10° (high disperson) and 2°+ 4° (intermediate dispersion) prisms. Of these 132 galaxies, the numbers detected on just high dispersion, just intermediate dispersion, and both high and intermediate dispersion plate pairs are 2, 4, and 21 respectively. It seems, therefore, that the detection limit does *not* depend strongly on our choice of prism dispersion. Other factors such as emulsion sensitivity, exposure time, sky transparency and particularly seeing are likely to affect the detection efficiency at least as much as prism choice.

2.5.2 Hα emission morphology

A comparison of emission morphology class (VC, C, N, D, VD) for the intermediate and high dispersion plates shows quite good agreement. For the 21 galaxies detected on both sets of plates, there is only a slight tendency for galaxies to be classified as more diffuse on the high dispersion plates, with mean difference $= 0.7 \pm 0.2$ classes. The final concentration parameter given in Table 2 was therefore taken to be the mean of the separate determinations.

2.5.3 Redshift measurements

In Paper I, a method was described for determining redshifts from two prism plates taken with the dispersion in opposite directions. Using this method on 10° prism data yielded a number of new redshifts and an error estimate of 200 km s^{-1} (1σ). Applying this method to 35 galaxies with known redshifts on the 2°+ 4° prism plates yields an error estimate of 270 km s^{-1} (1σ). Although this is less accurate than the 10° prism data (as expected) it is nevertheless sufficiently accurate to establish cluster membership. A few new redshifts measured this way are included in Table 2.

2.5.4 Hα equivalent widths and fluxes

Following plate digitization, it is possible to derive quantitative values for the equivalent width and flux of the Hα + [N II] emission, using the methods given in Paper I. For the present study, we have two main aims. First, we want to establish whether these methods can be applied to the lower dispersion prism combination. Secondly, we want to reconfirm that the method actually works, since there were previously only six photoelectric measurements with which to compare. Since then, more photoelectric measurements have been published, and our sample of emission line galaxies has grown, allowing a more thorough test of the method.

Measurements of Hα + [N II] equivalent width and flux for the

Table 3. Hα+ [N II] equivalent width and flux values.

CGCG	W_λ (Å)				$-\log f$ (erg cm^{-2} s^{-1})				$< W_\lambda >$	$< -\log f >$
no.	(2° + 4°)	(10°)	(KBS)	(GBK)	(2° + 4°)	(10°)	(KBS)	(GBK)	(Å)	(erg cm^{-2} s^{-1})
(1)	(2)	(3)	(4)	(5)	(6)	(7)	(8)	(9)	(10)	(11)
126.074	...	34	34	...	...	12.52	12.56	...	34	12.55
126.075	...	23	...	...	...	12.89	...	...	23	12.89
126.091	...	...	...	...	...	12.65	...	...	...	12.65
126.103	...	...	...	...	...	12.88:	...	...	...	12.88:
126.104	88	...	...	...	12.81	12.72	...	...	88	12.75
126.110	86	74	...	...	12.33	12.00	...	...	80	12.11
97.026	85	96	88	...	12.14	12.20	12.26	...	89	12.23
97.044	...	...	...	...	...	12.57:	...	...	...	12.57:
127.025A	...	...	22	...	...	...	12.66	...	22	12.66
127.025B	...	...	...	21	...	...	...	12.97	21	12.97
97.062	58		45	...	12.93	...	13.10	...	49	13.07
97.067	...	21:	...	...	...	12.63	...	...	21:	12.63
97.068	54	22	44	...	12.62	12.83	12.51	...	41	12.60
97.070	...	59:	...	53	...	12.14:	...	12.23	55	12.21
97.072	...	...	5	...	...	13.06:	13.50:	...	5	13.39:
97.073	...	...	80	...	...	12.84	12.84	...	80	12.84
97.079	...	...	145	...	...	12.54	12.64	...	145	12.61
97.087	84	65	61	...	12.43	12.23	12.19	...	68	12.23
97.091	21	17	23	...	12.86	12.92	12.74	...	21	12.79
97.092A	30	...	...	...	12.95	13.06	...	...	30	13.02
97.093	45	59:	...	...	12.95	12.95	...	...	52	12.95
97.114	60	79:	...	...	12.82	12.82	...	...	69	12.82
97.120A	...	...	4	...	...	...	13.20:	...	4	13.20:
97.121	...	...	0	...	...	...	...	...	0	...
97.122	41	40	46	...	12.82	12.65	12.65	...	43	12.67
97.125	26	29	...	...	13.04	13.13	...	...	27	13.10
97.129A	...	...	10	...	...	...	12.58	...	10	12.58
127.045	13	...	...	...	13.01	...	...	...	13	13.01
127.046	22	61[a]	...	11	13.20	13.05[a]	...	13.40	15	13.37
97.138	...	...	31	...	...	...	13.09	...	31	13.09
127.049	55	59	...	...	12.78	12.95	...	...	57	12.89
127.050	...	...	16	...	...	...	12.80	...	16	12.80
127.051A	...	38	...	26[b]	...	12.88	...	12.83[b]	30	12.84
127.052	11	...	...	...	12.83	...	...	...	11	12.83
127.054	...	...	5	...	...	...	13.00[c]	...	5	13.00[c]
127.055	40	43	...	...	12.68	12.85	...	...	41	12.79
97.149	...	...	...	13	...	...	...	13.38	13	13.38
127.058	36	...	...	...	13.10	...	...	...	36	13.10
127.068	...	...	...	26	...	...	...	13.14	26	13.14
127.071	73	72	...	52	12.68	12.72	...	12.83	62	12.79
127.073	...	...	3	...	...	...	...	...	3	...
127.074	37	45	...	...	12.82	12.75	...	...	41	12.77
97.168	78	...	...	...	13.05	...	...	...	78	13.05
127.082	...	...	22	...	...	...	12.86	...	22	12.86
127.095	...	...	15	...	...	...	12.63	...	15	12.63
127.100	...	...	10	...	...	...	13.14	...	10	13.14
97.180	...	...	...	...	...	13.03:	...	...	...	13.03:

[a] These values were omitted from the calculation of the weighted mean since they are clearly discrepant.
[b] The prism data clearly detect emission from the southern component, CGCG 127.051A, but not from the northern component, CGCG 127.051B. Although GBK quote $W_\lambda = 26$ Å for the north component, we assume that this refers to the southern component, CGCG 127.051A.
[c] Lower limit.

Explanations of columns in Table 3.
Column 1. CGCG number (Zwicky & Herzog 1963).
Columns 2–5. Global Hα + [N II] equivalent width values for the 2° + 4° prism combination (this paper); for the 10° prism (Paper I); from photoelectric data (Kennicutt et al. 1984 – KBS); and from photoelectric data (Gavazzi et al. 1991 – GBK), respectively.
Columns 6–9. Global Hα + [N II] flux values from the same sources as columns 2–5.
Column 10. Weighted mean value of global Hα + [N II] equivalent width.
Column 11. Weighted mean value of global Hα + [N II] flux.

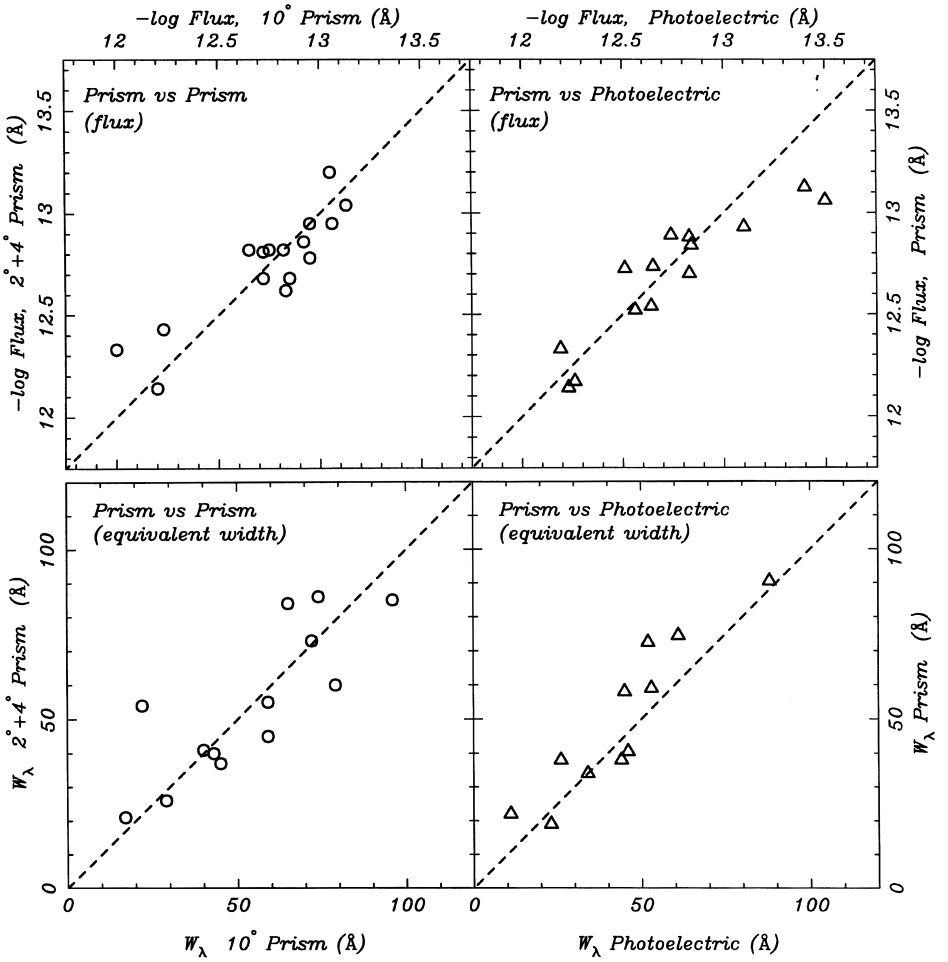

Figure 2. Comparisons of Hα equivalent width measurements (bottom pair) and Hα flux measurements (top pair) between the 2°+ 4° and 10° prisms (left side) and between prism and photoelectric measurements (right side).

high dispersion plates (B and C) were presented in Paper I and have not been repeated for the present study. Following the same methods, similar measurements were attempted for the emission line galaxies found on the intermediate dispersion plates (A and B). In practice, it is found that the intermediate dispersion data are more difficult to measure. The principal reason is that after compression to a 1D spectrum, the Hα emisson does not stand out as clearly above the continuum because the continuum is itself shorter. Nevertheless, for reasonably compact Hα at moderate redshifts (placing the emission away from the peak in the continuum distribution), measurements of equivalent width and flux are possible. Overall, the fraction of emission line galaxies with measureable equivalent width and flux drops from 55 and 95 per cent for the 10° prism to 44 and 58 per cent for the 2°+ 4° prism combination. Table 3 gives these values for the two prism configurations, as well as photoelectrically determined values from Kennicutt, Bothun & Schommer (1984) and Gavazzi, Boselli & Kennicutt (1991).

Fig. 2 (lower pair) shows comparisons of Hα equivalent width between the two prism configurations, and also between prism and photoelectric measurements. All values are taken from Table 3. Fig. 2 (top pair) shows similar plots for Hα flux measurements. Overall, there is good agreement with no systematic differences between either the two prism configurations, or between prism and photoelectric measurements. To quantify this, uncertain values and values derived from only a single plate were omitted from the following analysis. For equivalent width, comparison of the three sets of measurements gives estimated 1 σ errors of approximately 10, 10 and 7 Å from the 2°+ 4° prism (this paper), the 10° prism (Paper I), and the photoelectric measurements respectively. Using these error estimates, weighted mean equivalent width values were calculated and are listed in column 10 of Table 3. A similar analysis to provide error estimates for Hα flux is not possible because of possible correlated errors in the two prism measurements. However, comparison of the photoelectric fluxes together with three unpublished CCD flux measurements yield an error estimate of 0.07 in the log for these values. Comparison of photoelectric and prism measurements then gives estimated errors of 0.17 and 0.12 in the log for fluxes measured from 2°+ 4° and the 10° prism configurations respectively. Using these error estimates, weighted mean logarithmic flux values were calculated and are listed in column 11 of Table 3. Overall, then, when Hα equivalent widths and fluxes can be measured, it seems the quality of measurements from 2°+ 4° and 10° prism configurations is not significantly different.

2.6 Detection limits of the survey

2.6.1 Hα detection limits

In Paper I we were able to crudely define an Hα detection threshold

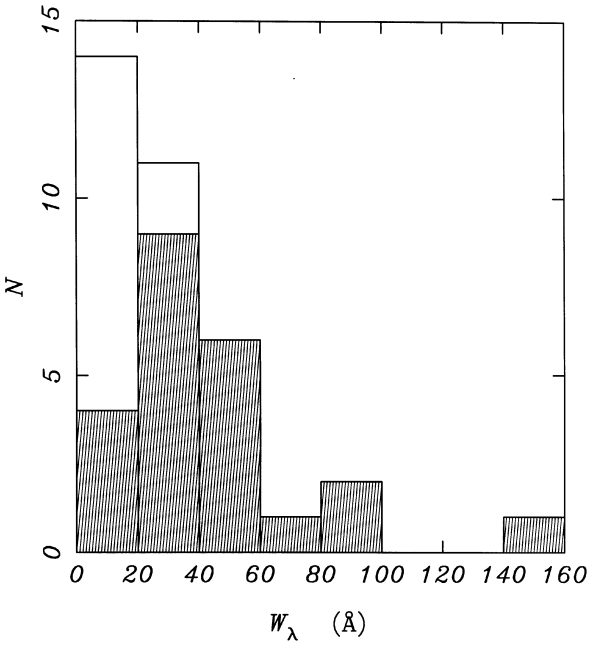

Figure 3. The distributions of photoelectrically determined Hα equivalent width for 35 CGCG galaxies falling on one or more prism plate pairs in Abell 1367 and Abell 1656. Detected galaxies (shaded) and undetected galaxies (unshaded).

for the prism technique, using photoelectric data on 15 galaxies which lay within our surveyed region. With more photoelectric measurements now available, and a wider region surveyed, we are able to improve our estimate for the Hα detection threshold. In total, we now have 35 CGCG galaxies with photoelectric measurements by Kennicutt et. al. (1984) or Gavazzi et al. (1991) which lie on one or more prism plate pairs in Abell 1367 (this paper) or Abell 1656 (Moss & Whittle, in preparation). Fig. 3 shows the distribution of photoelectrically determined Hα equivalent width for galaxies on our prism plates (whether detected in Hα or not). Detection is 90 per cent complete above 20 Å and 17 per cent complete below. In Paper I we also considered the distribution of equivalent width × flux as an improved measure of detection threshold. With our expanded data set, there is no clear gain in using this combined measure, and we adopt 20 Å as a useful guide to our completeness limit, with ∼20 per cent detection efficiency below this limit.

2.6.2 Hα detection dependence on magnitude

Table 4 gives the total number of CGCG galaxies of type S0/a and later in four magnitude bins ($m_p = 13.6 - 15.7$), together with the corresponding number of Hα detections. A simple comparison of these two numbers is insufficient to study the magnitude dependence of Hα detection because of the dependence on Hubble type.

Table 4. Detection of emission-line galaxies with magnitude (types S0/a and later).

	Magnitude interval (m_p)			
	13.6–14.2	14.3–14.7	14.8–15.2	15.3–15.7
N(total)	7	14	13	62
ELGs (observed)	4	5	4	19
ELGs (expected)	3	5	4	20

To allow for this, we use the detection efficiencies for each Hubble type (see Section 3.1 below) and the Hubble type distributions within each magnitude bin (from Table 2), to calculate an expected number of detections for each magnitude bin. The fact that the expected numbers detected agree well with the actual numbers detected suggests the detection efficiency is independent of magnitude for each Hubble type. Since the cluster galaxies are all at the same redshift, we conclude that there is no significant dependence of Hα detection on absolute magnitude in the range $-21.5 \leq M_B \leq -19.5$ (corresponding to $m_p = 13.6 - 15.7$ using $H_0 = 50\,\mathrm{km\ s^{-1}\ Mpc^{-1}}$). This agrees with the earlier finding of Kennicutt & Kent (1983) that the equivalent width of Hα for Sc and SBc field galaxies is independent of absolute magnitude in the range $-23 \leq M_B \leq -18$.

What about Hα detection in galaxies fainter than $m_p = 15.7$? In Paper I, we surveyed the overlap region of plates C and D for *all* emission line galaxies, and found 11 fainter than $m_p = 15.7$ (i.e. not in the CGCG catalogue). Of these, Kraft (1978) gives magnitudes for six, of which four (ELG nos. 11, 23, 27 and 35) are fainter than $m_p = 16.2$. Thus a maximum of seven galaxies are detected in the magnitude interval $15.8 \leq m_p \leq 16.2$. By extrapolation of the integrated counts for CGCG galaxies in the range $13.7 \leq m_p \leq 15.7$, we estimate a total of 62 galaxies in the magnitude interval $15.8 \leq m_p \leq 16.2$. If these galaxies have the same Hubble type distribution as galaxies in the magnitude interval 15.3–15.7, then we expect to detect in Hα a total of 19. Since we only detect at most seven, we conclude that our detection efficiency drops sharply below the magnitude limit of the CGCG catalogue. Although this could reflect a genuine decrease in star formation in the fainter galaxies, we suspect it results from the detection limit of the photographic plate.

2.7 Refined galaxy samples

Although our original survey sample was all CGCG galaxies falling on any prism plate, we have selected somewhat modified subsamples for some of the analyses presented below. For example, the most homogeneous sample of all Hubble types includes all CGCG galaxies falling on either plate pair, excluding members of double CGCG galaxies the estimated magnitude of which is fainter than m_p = 15.7. This sample contains 174 galaxies, of which 34 are emission-line galaxies, and is used in the analysis of Hα detection dependence on Hubble type (Section 3.1, below). As found in the Hubble-type analysis, very few E or S0 galaxies are detected in Hα, and so a 'spiral sample' can be defined by including only galaxies of type S0/a and later. This sample was used to study the Hα detection dependence on galaxy magnitude (Section 2.6.2). The sample was further reduced by excluding all galaxies with known redshift greater than 3σ from the cluster mean. Finally, since our principal interest is the relation of star formation to various galaxy properties and environment, the Seyfert galaxy CGCG 126.110 was also excluded. This spiral sample now includes 80 galaxies of which 26 (32 per cent) are emission line galaxies. This sample is used in the analysis of Hα detection in barred and disturbed galaxies (Section 3.2), and the comparison of cluster and field galaxies (Section 4).

3 Hα EMISSION AND GALAXY MORPHOLOGY

3.1 Hα detection dependence on Hubble type

Unlike the samples used in Papers II and IV, which are restricted to spirals, the present sample provides an important opportunity to

Table 5. Frequency of emission detection with galaxy type.

Type	*N*	Emission
E, E–S0	30	0%
S0	48	4%
S0/a	21	14%
Sa, Sab	34	32%
Sb, Sbc	17	53%
Sc, Sc–Irr	14	36%
S...	10	40%

study the detection frequency of Hα emission along the entire Hubble sequence. Table 5 gives these frequencies for the full CGCG sample. Clearly, elliptical and S0 galaxies are rarely if ever detected whilst $\sim$30$-$50 per cent of all spirals are detected, and the intermediate class of S0/a galaxies has an intermediate detection fraction. The overall trend is probably best described as rapidly rising from zero to $\sim$35 *percent* in early spirals, then approximately constant along the spiral sequence (though there are too few mid- and late-type spirals to be confident of this, see Paper IV for a more complete description of the spiral sequence). This behaviour agrees qualitatively with that found for field galaxies by Kennicutt & Kent (1983) and supports, therefore, our basic detection criteria and Hubble type classifications. At this stage, however, we choose not to compare in detail with the Hubble type dependence found by Kennicutt & Kent, because the samples and detection methods are too different.

3.2 Hα detection for disturbed and barred galaxies

In relating the detected emission to disturbance and bars, it is important to distinguish between diffuse and compact Hα emission. Using the concentration parameter described in Section 2.4, *diffuse* emission is described by the two classes, D (diffuse) and VD (very diffuse), while *compact* emission is described by the other three classes, VC (very concentrated), C (concentrated) and N (normal). Of the 26 emisson line galaxies in the final spiral sample, 17 show compact emission and nine show diffuse emission. We refer to these groups as ELG(all), ELG(comp), and ELG(diff).

We first consider the relation between Hα detection and disturbed morphology. Kendall rank tests yield correlation significance levels of 3.1σ, 5.4σ, and $-$2.4σ for the dependence of ELG(all), ELG(comp), and ELG(diff) on galaxy disturbance (where $-$2.4σ signifies a weak *anti*-correlation between diffuse emission and galaxy disturbance). These results reinforce those from Paper II, and confirm the very significant tendency for galaxies with compact emission to be disturbed, while galaxies with diffuse emission have no tendency to be disturbed. For the present sample, 71 per cent of galaxies with compact emission are disturbed (12 of 17), while only 15 per cent of galaxies which do not have compact emission are disturbed (11 of 74).

Turning to the relation between Hα detection and the presence of a bar, we find Kendall rank tests yield correlation significance levels of 1.7σ, 3.0σ, and $-$1.1σ for the dependence of ELG(all), ELG(comp), and ELG(diff) on bars. Taken at face value, there is a moderate tendency for galaxies with compact emission to have bars. However, because of the strong association between compact emission and disturbance, it is prudent to reanalyse the relation having excluded disturbed galaxies. Although this yields a result of only 1.3σ significance, it is difficult to interpret because the sample size is now rather small. A similar analysis for a larger sample (Paper IV) gives a somewhat higher significance. We conclude that there may be a weak tendency for compact emission to be associated with bars, independently of its association with disturbance.

As discussed in Paper II, these results support the idea that diffuse emission results from normal star formation in spiral discs, while compact emission results from a burst of star formation in the centre of the galaxy, principally associated with a disturbed galaxy morphology. The disturbed galaxy morphology is most likely the result of tidal forces, whether from galaxy–galaxy or cluster–galaxy interactions. It is well known that such tidal forces can trigger star formation, particularly in the nucleus of a galaxy (e.g. Noguchi 1988; Barnes & Hernquist 1991).

The question remains as to whether these tidally induced starbursts are the result of galaxy–galaxy or cluster–galaxy interactions. Before discussing this question, it is necessary to compare detected emission in cluster and field spirals (see Section 4.2). The possible mechanisms for tidal triggering of nuclear starbursts in the present galaxy sample will be discussed in Section 4.3.

4 CLUSTER–FIELD COMPARISON

4.1 Cluster spiral sample

One of the main aims of our objective prism Hα survey is to compare star formation rates for spiral galaxies in clusters and spiral galaxies in the field. In Paper II, we were only able to do this by constructing a field sample using the photoelectric measurements of Kennicutt & Kent (1983). In the present data set, however, the richness of the region and the large area surveyed allow us to construct our own field sample, using the outer parts of the surveyed area. This is to be preferred, in principle, because the survey methods are then identical for the cluster and field samples.

A question then arises: which galaxies are 'cluster' galaxies, and which are 'field' galaxies ? In general, it is not sufficient simply to select cluster galaxies from within the conventional cluster boundary (1.0 $r_{\rm A}$), since many of these are likely to be superposed from the general supercluster field. This is especially true for spirals, which are less concentrated towards the cluster centre than elliptical or S0 galaxies, as illustrated in Fig. 4 for Abell 1367.

To select a sample of cluster spirals, we first assume that galaxies lying outside 1.5 $r_{\rm A}$ belong to the field. The surface density of all CGCG galaxies in the region 1.5–3.0 $r_{\rm A}$ was evaluated from the Zwicky catalogue, and converted to a surface density of spirals assuming the spiral fraction was the same as our surveyed region outside 1.5 $r_{\rm A}$ (taking Hubble types from Table 2). This field spiral surface density was used to evaluate how many field spirals are expected to fall in three cluster zones, 0.0–0.5 $r_{\rm A}$, 0.5–1.0 $r_{\rm A}$, 1.0–1.5 $r_{\rm A}$. We estimate the percentage contamination by field spirals in these three cluster zones to be in the ranges 14 $\pm$ 6, 109 $\pm$ 30 and 83 $\pm$ 18 per cent respectively. This now allows us to construct three samples : a 'predominantly cluster' sample ($n = 24$, $r < 0.5$ $r_{\rm A}$); a 'predominantly field' sample ($n = 56$, $r > 0.5$ $r_{\rm A}$); and a 'pure field' sample ($n = 29$, $r > 1.5$ $r_{\rm A}$).

4.2 Emission in cluster and field spirals

In order to compare Hα emission from cluster and field spirals for Abell 1367, a further sample modification was made to ensure that only strong star formation is included: galaxies with Hα equivalent

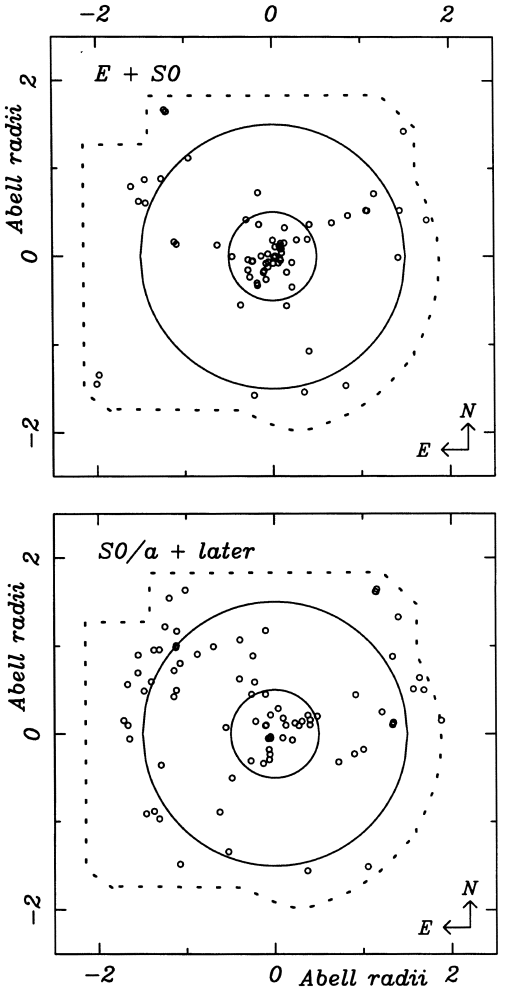

Figure 4. Distributions of surveyed CGCG galaxies of types E and S0 (upper panel), and types S0/a and later (lower panel). Both panels are drawn with the same orientation and scale. Circles in each panel are centred on Abell 1367, with radii, $r = 0.5\,r_A$ and $1.5\,r_A$. The boundary of the surveyed region is shown by the dashed line.

widths less than 20 Å were not considered as detections (CGCG 127.095, 127.045, 97.072). The first row of Table 6 compares the detection efficiencies for the 'predominantly cluster' and 'predominantly field' spiral samples, of all types. Clearly, a higher percentage (46 per cent) of cluster spirals are detected with strong emission, compared to the percentage (21 per cent) of field spirals with strong emission, although a χ^2 test shows only modest significance for this difference (2.2σ). Nevertheless, there is no evidence from these data for any *lessened* emission for cluster spirals compared to field spirals.

The remaining rows of Table 6 compare the percentages of cluster and field spirals with strong emission for various spiral types. Again, there is no evidence for any lessened emission in cluster galaxies compared to field galaxies of the same types. Indeed, within the limits of these rather small sub-samples, it seems that late-type cluster spirals have a *higher* fraction in emission than late-type field spirals (χ^2 test gives 2.7σ significance).

These results may be compared with our cluster/field analysis in Paper II, which found enhanced/similar emission in early-/mid-type cluster spirals (as found here) but significantly found *reduced* emission in late-type cluster spirals (opposite to the result here). There are two effects which may have contributed to this last

Table 6. Comparison of Hα emission in cluster and field spirals (types S0/a and later).

Sample	Cluster ($r \leq 0.5\,r_A$)		Field ($r > 0.5\,r_A$)	
	n_t	%($W_\lambda \geq 20$ Å)	n_t	% ($W_\lambda \geq 20$ Å)
All spirals	24	46%	56	21%
S0/a, Sa	11	36%	29	10%
Sab,Sb	6	33%	11	36%
Sbc + later	4	100%	10	20%

difference. First, as discussed in Paper II, it is possible that our detection sensitivity for diffuse Hα emission in the late-type spirals (which have lower mean surface brightness) is lower than the photoelectric photometry of Kennicutt & Kent (1983), which was used to measure the field sample. Secondly, the sample of cluster spirals used in Paper II included the outer regions of the clusters where significant field galaxy contamination may be expected. In contrast, the present study not only uses the same detection method for cluster and field samples, it also considers projection effects more carefully when deciding which galaxies are cluster and which are field. We expect, therefore, the present study to give the more reliable result.

In fact, our present analysis still does not use an ideal field sample. Not only are there likely to be some cluster spirals projected on to the region outside $0.5\,r_A$, but Abell 1367 is an irregular and unrelaxed cluster in which one finds sub-cluster groupings in the immediate surrounding region. For this reason, a more conservative approach is to omit all galaxies in the intermediate region $0.5\,r_A \leq r \leq 1.5\,r_A$ and construct a 'pure field' sample from spirals outside $1.5\,r_A$ (this approximately halves the field sample size).[1] Using these relatively uncontaminated cluster and field samples, a χ^2 analysis which compares the fraction of Hα detections in the cluster and field gives the following results: for ELG(all) there is a fairly significant increase in the cluster (2.9σ, 46 versus 10 per cent); which is almost entirely a result of the excess in galaxies with compact emission (3.6σ, 38 versus 0 per cent); while there is no difference for galaxies with diffuse emission (0.3σ, 8 versus 10 per cent, samples of $n = 24$ for cluster and $n = 29$ for field; the corresponding results for the previous field sample with $n = 56$ were 2.2σ, 2.5σ, and 0.0σ, respectively). The distribution of diffuse and compact Hα emitting galaxies across the cluster and field are shown in Figs 5 and 6 respectively.

Thus we find a significant enhancement of compact emission in cluster galaxies compared to field galaxies of similar type. As discussed above, compact emission is strongly associated with disturbed galaxy morphology and, hence, with tidal disturbance. This in turn suggests, perhaps not surprisingly, that tidally induced star formation occurs with higher frequency within the cluster environment than in the field.

4.3 Mergers, harassment, galaxy–galaxy and cluster–galaxy interactions

With evidence for enhanced tidally triggered star formation in cluster galaxies, we now ask whether it is possible to identify the source of the tidal perturbations. There are several possibilities to consider. First, at low relative velocity a galaxy may interact

[1] It should be understood that in the present context 'pure field' refers to the supercluster environment, and this may not correspond to a true field sample in the strictest sense.

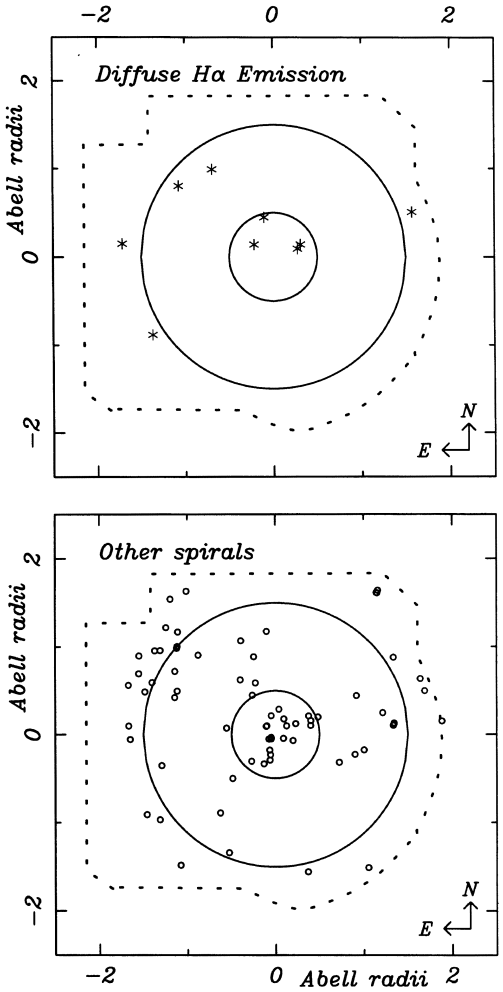

Figure 5. Distributions of galaxies of types S0/a and later showing diffuse emission (upper panel) and without diffuse emission (lower panel). Figures and circles are drawn as in Fig. 4.

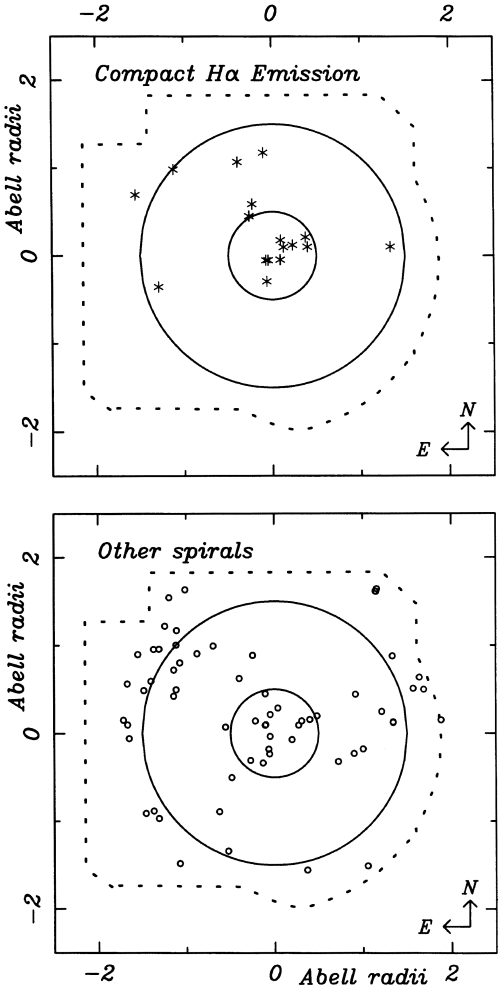

Figure 6. Distributions of galaxies of types S0/a and later showing compact emission (upper panel) and without compact emission (lower panel). Figures and circles are drawn as in Fig. 4.

strongly with a nearby companion. Secondly, at higher relative velocity, a galaxy may be 'harassed' as it flies past other galaxies in the cluster. Thirdly, a galaxy can be disturbed by the tidal field of the cluster as a whole. To some extent these can be distinguished observationally from one another. Obviously, for the first case one expects to see the companion galaxy nearby, although if the interaction has progressed to the point of merger the system may appear isolated and probably disturbed. Isolated disturbed spirals are also candidates for 'harassed' galaxies, which can move well past their encounter before their disturbance becomes visible (Moore et al. 1996). Galaxies perturbed by the cluster potential are only found close to the cluster core where the tidal field is strongest (Byrd & Valtonen 1990). As with harassment and minor mergers, these galaxies are likely to look disturbed yet have no true companions.

We now turn to our data to assess the evidence for each of these possible mechanisms. First, short-range tides are clearly important in some cases. For example, there are a number of very close emission line systems which may be ongoing mergers. CGCG 97.079 is a double galaxy with continuum and Hα nuclei separated by only $\sim$9 arcsec. Three galaxies with compact Hα emission appear single on direct plates but double on prism plates (CGCG 127.071, CGCG 126.110, CGCG 127.058). The prism plates are less deep, revealing more clearly the double nuclear morphology which in one case (CGCG 126.110) is confirmed by CCD images showing two nuclear components separted by 6.6 arcsec (Keel 1996). Interestingly, these three galaxies are classed as disturbed, possibly disturbed, and undisturbed respectively, showing that although some ongoing mergers leave visual clues, some do not, possibly because of the smallness of the merging companion. Clearly, CCD imaging would help reveal these more hidden signs of tidal perturbation.

Apart from these individual cases, it is also possible to test statistically whether galaxies with Hα emission are associated with tidally interacting companion galaxies. In fact, a Kendall rank test finds no statistically significant association between Hα emission and the presence of a nearby companion, as parametrised by C, C: or C::. However, in a cluster environment this parameter is particularly susceptible to projection effects. We therefore define a more restrictive parameter called 'tidal companion', TC. This is assigned if a galaxy has both a nearby companion *and* appears disturbed (it has an uncertainty rank equal to the lowest of the individual uncertainty ranks for C and D, eg C: and D give TC:). The TC parameter helps to clarify several things. First, it helps to screen out projected neighbours. This is effective over most of the surveyed region where the chance association of D and C is quite low, but

may be less effective in the cluster core where projection effects are increasingly dominant. Secondly, it screens out galaxies which have a real companion but are not, for whatever reason, disturbed by it. Thirdly, it isolates only those disturbances which are probably caused by a nearby companion. Thus, while not perfect, the TC parameter probably targets tidally induced disturbance by a near neighbour quite effectively.

A Kendall rank test for the association between Hα emission and TC yields correlation significance levels of 3.2σ, 5.4σ, and -2.3σ for ELG(all), ELG(comp), ELG(diff) respectively. Thus, there is a very significant association for galaxies with compact emission, but not for galaxies with diffuse emission. Explicitly, of the 17 galaxies with compact emission, nine have tidal companions while a further two have double nuclei suggesting a merger. Allowing for the four galaxies in the cluster core ($r < 0.25\ r_A$) for which the TC may be spurious, we therefore estimate $\sim$40$-$65 per cent of the galaxies with compact emission are triggered by tidal interactions with neighbour galaxies. This is a lower limit since closer examination of the other galaxies may reveal evidence of minor mergers.

Turning to the possibility of tidal perturbation by the cluster potential, we note that galaxies with compact emission are not *only* found in the central regions, where theory predicts they should lie (e.g. $\lesssim 0.25\ r_A$, Byrd & Valtonen 1990). However, while our data do not support the cluster potential as a dominant tidal trigger, we cannot rule out its importance at least in the central regions. For example, of the five galaxies with compact emission in the cluster core, four are classified as disturbed (97.087, 97.093, 97.114, 97.125) and comprise possible candidates for perturbation by the cluster tidal field. As it happens, these four disturbed galaxies also appear to have companions (classed C or C:), raising the possibility of neighbour interaction rather than cluster interaction. In the core, however, projection effects are more important and without further information we cannot be confident as to which of these effects is occurring.

In assessing the importance of harassment in triggering star formation, we must also consider the isolated but disturbed galaxies. From our full CGCG sample, the fraction of disturbed galaxies with no apparent companions (i.e. not classed as C, C:, or C::) increases from $\sim$25 per cent for D and D: to about $\sim$50 per cent for D::, totalling $\sim$15 galaxies which are possible candidates for galaxy harassment. Of these, only three have compact emission (97.062, 97.079, 97.122) all of which are found within the cluster, and one of which (97.079) is a probable merger. If we add to these remaining two, the four core galaxies whose companions may be projected (see above), we have up to six candidates for compact emission triggered by galaxy harassment, or $\sim$66 per cent of the cluster galaxies ($r < 0.5\ r_A$) with compact emission. This is an upper limit since the core galaxies may indeed have companions and the isolated disturbed galaxies may be minor mergers.

In summary, we cannot rule out any of the processes discussed above. Certainly, interaction with near neighbours seems to play an important role, given the high fraction of galaxies with compact emission which are classed as TC. Conversely, it seems that interaction with the cluster potential is *not* the dominant process, though we find several candidate galaxies for this type of interaction in the core. We also find possible candidates for triggering by galaxy harassment. To some extent, our inability to distinguish between these mechanisms stems from the ambiguity of projection effects in the innermost regions of the cluster.

5 CONCLUSIONS

We have used an objective prism technique to survey CGCG galaxies in and around the cluster Abell 1367 for Hα emission. We provide information on Hubble type, galaxy disturbance, galaxy companions, Hα emission and Hα morphology, for 217 galaxies out to $\sim$2 Abell radii ($\sim 2\overset{\circ}{.}5$, $\sim$6 Mpc). First, we explore and confirm the use of the $2^\circ + 4^\circ$ prism for our survey as an alternative to the 10° prism. The measured detecton limits, Hα morphology, redshifts, fluxes and equivalent widths are all comparable between the two prisms, though as expected the quantitative measures are slightly less accurate for the $2^\circ + 4^\circ$ prism. Secondly, we characterize the detection limit of the technique, showing that it is approximately complete above $\sim$20 Å global equivalent width, and approximately independent of apparent and absolute magnitudes in the range $m_p < 15.7$ and $-21.5 < M_p < -19.5$. Thirdly, we study the dependence of Hα detection on Hubble type, galaxy disturbance and bars. As expected, the detection rate is low for elliptical and S0 galaxies, intermediate for S0/a, and and high ($\sim$30$-$50 per cent) for spirals. There is a strong tendency for galaxies with compact emission to be disturbed, and there may be a weak tendency for these galaxies to be barred. These dependencies are not found for galaxies with diffuse emission.

Finally, our principal scientific aim is to compare the Hα detection rates for spirals (type S0/a and later) in the cluster and in the field, at least as found for the single cluster Abell 1367. We extend the analysis from Paper II in three imporatant ways: (a) by surveying a larger area around the cluster we can construct our own field sample; (b) the Hα detection method is the same for the cluster and field samples; (c) by considering field contamination more carefully, we can construct cleaner cluster and field samples. We find a much higher fraction of spirals detected in Hα in a 'predominantly cluster' sample ($r < 0.5\ r_A$) compared with a 'predominantly field' sample ($r > 0.5\ r_A$), though the result is of low statistical significance (e.g. 46 versus 21 per cent for cluster and field spirals, significance level 2.2σ). This effect appears to be independent of spiral stage, with similar results for early-, mid- and late-type spirals. These results are strengthened considerably when we use a 'pure field' sample ($r > 1.5\ r_A$, 46 versus 10 per cent, significance 2.9σ), where we learn that the effect occurs only in the galaxies with compact emission (38 versus 0 per cent, significance 3.6σ).

We interpret these results in the following way. Compact emission results from tidal perturbations and is enhanced in the cluster environment, while diffuse emission is more normal and shows no strong cluster/field difference. The tidal perturbations arise at least in part from interactions with near neighbours, although we also find candidate objects near the cluster core which may be perturbed by the overall cluster tidal field, and candidate objects for a higher speed 'harassment' interaction between galaxies.

ACKNOWLEDGMENTS

CM thanks the Vatican Observatory Research Group, University of Arizona, and MW thanks the Institute of Astronomy, Cambridge for hospitality during the course of this project. Observations were made with the Burrell Schmidt Telescope of the Warner and Swasey Observatory, Case Western Reserve University. This research has made use of the NASA/IPAC Extragalactic Database (NED) which is operated by the Jet Propulsion Laboratory, California Institute of Technology, under contract with the National Aeronautics and Space Administration.

REFERENCES

Abell G. O., 1958, ApJS, 3, 211

Barnes J. E., Hernquist L. E., 1991, ApJ, 370, L65
Biviano A., Katgert P., Mazure A., Moles M., den Hartog R., Perea J., Focardi P., 1997, A&A, 321, 84
Byrd G., Valtonen M., 1990, ApJ, 350, 89
Couch W. J., Ellis R. S., Sharples R. M., 1994, ApJ, 430, 121
de Vaucouleurs G., 1959, in Flügge S., ed., Handbuch der Physik, Vol. LIII. Springer-Verlag, Berlin, p. 275
de Vaucouleurs G., 1974, in Shakeshaft J.R., Proc. IAU Symp. 58, The Formation and Dynamics of Galaxies. Reidel, Dordrecht p.1
de Vaucouleurs G., de Vaucouleurs A., Corwin H. G., Buta R. J., Paturel G., Fouquè P., 1991, Third Reference Catalogue of Galaxies, Vol. II. Springer-Verlag, New York
Donas J., Buat V., Milliard B., Laget M., 1990, A&A, 235, 60
Dressler A., Thompson I. B., Schectman S. A., 1985, ApJ, 288, 481
Dressler A., Oemler A., Butcher H. R., Gunn J. E., 1994, ApJ, 430, 107
Gavazzi G., Contursi A., 1994, AJ, 108, 24
Gavazzi G., Randone I., 1994, A&AS, 107, 285
Gavazzi G., Boselli A., Kennicutt R., 1991, AJ, 101, 1207
Gavazzi G., Randone I., Branchini E., 1995, ApJ, 438, 590
Gisler G. R., 1978, MNRAS, 183, 633
Hill J. M., Oegerle W. R., 1993, AJ, 106, 831
Huchra J. P., Geller M. J., Clemens C. M., Tokarz S. P., Michel A., 1992, CfA redshift catalogue, Bull. Inf. Cent. Données Stellaires, 41, 31
Kauffmann G., 1995, MNRAS, 274, 153
Karachentsev I., Lebedev V., Shcherbanoversuskij A., 1985, Bull. Inf. Cent. Données Stellaires, 29, 87
Keel W. C., 1996, AJ, 111, 696
Kennicutt R. C., Kent S. M., 1983, AJ, 88, 483
Kennicutt R. C., Bothun G. D., Schommer R. A., 1984, AJ, 89, 1279
Kinman T. D., 1984, in Cappacioli M., ed., IAU Colloq. 78, Astronomy with Schmidt-type Telescopes. Reidel, Dordrecht, p. 409
Kraft R., 1978, PhD thesis, Univ. of Cambridge
Lavery R. J., Henry J. P., 1988, ApJ, 304, L5
Lu N. Y., Hoffman G. L., Groff T., Roos T., Lamphier C., 1993, ApJS, 88, 383
Moore B., Katz N., Lake G., Dressler A., Oemler A., 1996, Nat, 379, 613
Moss C., Whittle M., 1993, ApJ, 407, L17 (Paper II)
Moss C., Whittle M., Irwin I. J., 1988, MNRAS, 232, 381 (Paper I)
Nilson P., 1973, Uppsala General Catalogue of Galaxies. Uppsala Astr. Obs. Ann., 6
Noguchi M., 1988, A&A, 203, 259
Oemler A., 1974, ApJ, 194, 1
Oemler A., Dressler A., Butcher H. R., 1997, ApJ, 474, 575
Osterbrock D. E., 1960, ApJ, 132, 325
Paturel G., Fouqueè P., Bottinelli L., Gougenheim L., 1989, Catalogue of Principal Galaxies. Observatoire de Lyon, Lyon
Sandage A., Tammann G. A., 1981, Carnegie Inst. Washington Publ. No. 635
Scodeggio M., Gavazzi G., 1993, ApJ, 409, 110
Struble M. F., Rood H. J., 1987, ApJS, 63, 543
Thompson L. A., 1988, ApJ, 324, 112
Tifft W. G., 1978, ApJ, 222, 54
Zabludoff A. I., Huchra J. P., Geller M. J., 1990, ApJS, 74, 1
Zabludoff A. I., Geller M. J., Huchra J. P., Vogeley M. S., 1993, AJ, 106, 1273
Zwicky F., Herzog E., 1963, Catalogue of Galaxies and Clusters of Galaxies, Part II. California Institute of Technology Press, Pasadena CA

This paper has been typeset from a TEX/LATEX file prepared by the author.